Experimental Results for OFDM WiFi-Based Passive Bistatic Radar

P. Falcone, F. Colone, C. Bongioanni, P. Lombardo
INFOCOM Dept. - University of Rome "La Sapienza"
Rome, Italy
{falcone, colone, bongioanni, lombardo}@infocom.uniroma1.it

Abstract— **In this paper the practical feasibility of a WiFi transmissions based passive bistatic radar (PBR) is analyzed. The required data processing steps are described there including the adopted techniques for: (i) the control of the signal Ambiguity Function usually yielding a high sidelobe level and (ii) the removal of the undesired signal contributions which strongly limit the useful dynamic range. The performance of the conceived system is evaluated with reference to typical signals broadcasted by a IEEE 802.11 access point exploiting an OFDM modulation. The achievable results are presented against a real data set collected by an experimental setup. This allowed us to preliminarily demonstrate the potentialities of a WiFi-based PBR for local area surveillance applications.**

I. INTRODUCTION

In recent years the use of Passive Bistatic Radar (PBR) for surveillance purposes has received renewed interest, [1]. PBR exploits existing illuminators of opportunity to perform target detection which results in the exciting possibility of low cost surveillance, reduced pollution of the e.m. environment, etc.

Among all the available emitters, broadcast transmitters represent some of the most attractive choices for long-range surveillance applications, owing to their excellent coverage. A number of studies have looked at the use of analogue signals such as FM and HF radio and UHF television broadcasts, [2-4], as well as digital transmissions such as DAB and DVB, [5-6]. In the above applications, PBR is rapidly reaching a point of maturity; even though there are still many challenges to be solved involving both technology development and processing techniques, PBR practical feasibility for long range surveillance has been well established.

With reference to local area monitoring applications, aiming at the detection and localization of designated human beings or man-made objects within short ranges, wider bandwidth signals of opportunity should be exploited to achieve the required range resolution. To this purpose wireless Local Area Network (LAN) transmissions might be considered, [7-8]. Wireless networking applications are proliferating at a very rapid rate for both commercial and private use. WiFi is one of the most popular technologies based on the IEEE 802.11 Standard, [9], which offers reasonable bandwidth and coverage with a wide accessibility.

A number of standards have been developed for the WiFi transmissions, among which the three commonly deployed versions: 802.11a, 802.11b, and 802.11g. According to the standard's physical layer specifications, in typical operation modes, a WiFi access point (AP) may broadcast a mix of signals based on different modulations and coding schemes. Therefore, it might act as an ideal illuminator of opportunity for short range detection and surveillance using the PBR principle. In [10] a preliminary analysis of the potentialities of a WiFi-based PBR has been presented with reference to Direct Sequence Spread Spectrum (DSSS) modulated signals.

In this paper the practical feasibility is demonstrated for a WiFi-based PBR exploiting the OFDM (Orthogonal Frequency-Division Multiplexing) waveforms with wider frequency bandwidth. To this purpose we show the experimental results obtained within a research project carried out at the InfoCom Dept. - Univ. of Rome "La Sapienza". The performance of the conceived system is evaluated based on an experimental setup developed and fielded in different operational scenarios. The developed signal processing techniques are described which have been optimized to cope with the characteristics of the OFDM-WiFi waveforms of opportunity in order to obtain an effective removal of the disturbances limiting target detection.

The paper is organized as follows. In Section II the main characteristics of IEEE 802.11 Standard are summarized and the Ambiguity Function (AF) of a typical OFDM frame is evaluated. In Section III the main data processing steps are described, including the adopted disturbance cancellation algorithm and the exploited techniques for AF sidelobes control. In Section IV the experimental setup is described while Section V reports our experimental results. Finally, our conclusions are drawn in Section VI.

II. THE IEEE 802.11 STANDARD AND SIGNAL AF

A number of 802.11 standards have been developed and further versions are being conceived. Among the most commonly deployed, 802.11a is only adopted in the US Regulation Domain, while 802.11g represents the 3rd

978-1-4244-5812-7/10/$26.00 ©2010 IEEE

generation of the standard after 802.11 and 802.11b and maintains a full compatibility with the older standards. These standards allow different data rates and operate according to different frequency channels plans. Moreover, there are a number of formats specified for the data unit based upon the IEE standard Physical Layer Convergence Protocol (PLCP). The transmission is of a pulsed type, with varying and unpredictable pulse durations depending on the PLCP Protocol Data Unit (PPDU) format and on the data frame size. The different data rates are achieved by exploiting different modulations/coding schemes according to the physical layer specification adopted by each standard. The main modulations are either DSSS or OFDM with data rates between 1 and 54 Mbps. DSSS is the most common modulation, with OFDM dominating at higher data rates. Moreover, an IEEE 802.11 AP periodically transmits a regular Beacon signal broadcasting its presence and channel information.

It is clear that the overall WiFi waveforms characteristics are complex and strongly time-varying, which affects the performance of a PBR based on them. A detailed analysis of the WiFi signal AF characteristics has been presented in [7] distinguishing between different signal types based on different modulations and coding schemes. Moreover the practical feasibility of a PBR based on WiFi DSSS modulated signals has been preliminary demonstrated in [10] where proper processing strategies have been proposed for the signal AF control. To complete the picture, the following analysis is focused on WiFi signals exploiting OFDM modulation.

In this case, the complex baseband signal pulse is composed of contributions from several OFDM symbols, [9]:

$$s(t) = s_{PREAMBLE}(t) + s_{SIGNAL}(t - t_S) + s_{DATA}(t - t_D) \quad (1)$$

where t_S=16μs, and t_D=20μs. The generic sub-frame $s_{SF}(t)$ is constructed as an inverse Fourier transform of a set of coefficients d_k which can be data, pilots, or training symbols:

$$s_{SF}(t) = w_{\Delta T}(t) \sum_{k=-N_{ST}/2}^{N_{ST}/2} d_k \cdot \exp\left[j2\pi k\Delta f\,(t - T_G)\right] \quad (2)$$

where

- N_{ST}=52 is the total number of sub-carriers with a sub-carrier frequency spacing equal to Δf=0.3125 MHz=20MHz/64 (T_{FFT}=1/Δf =3.2 μs is the period of the resulting waveform); notice that the central carrier (k=0) is never used (d_k=0);
- $w_{\Delta T}(t)$ is a time-windowing function of duration ΔT which may extend over multiple periods T_{FFT} of the Fast Fourier Transform (FFT).
- T_G is the guard interval; shifting the time by T_G creates the "circular prefix" used in OFDM to avoid inter-symbol interference (ISI) from the previous frame. Three kinds of T_G are defined: for the short training sequence (0 μs), for the long training sequence (T_{GI2}=1.6 μs), and for data OFDM symbols (T_{GI}=0.8 μs).

Specifically, the Preamble field is used for synchronization. It consists of 10 short symbols and two long symbols. The Short Training sequence is given by:

$$s_{SHORT}(t) = w_{\Delta T_{SHORT}}(t) \sum_{k=-N_{ST}/2}^{N_{ST}/2} S_k \cdot \exp\left[j2\pi k\Delta f\, t\right] \quad (3)$$

where the elements of the sequence S_k (k=-26,..,26) are defined in [9] and are non-zero only at indices that are a multiple of 4. Thus only 12 sub-carriers are actually used which results in a periodicity of $T_{FFT}/4$ = 0.8 μs. The interval ΔT_{SHORT} is equal to ten 0.8 μs periods (i.e., 8 μs) and thus consists of 10 repetitions of the short training symbol.

The Long Training sequence is given by:

$$s_{LONG}(t) = w_{\Delta T_{LONG}}(t) \sum_{k=-N_{ST}/2}^{N_{ST}/2} L_k \cdot \exp\left[j2\pi k\Delta f\,(t - T_{GI2})\right] \quad (4)$$

where the elements of the sequence L_k (k=-26,..,26) are defined in [9]. Two and a half periods of the long sequence are transmitted for improved channel estimation accuracy, yielding $\Delta T_{LONG}=T_{GI2}+2T_{FFT}$=8 μs.

The Signal OFDM symbol follows the preamble field and is used to carry control information, such as frame length and data rate. Its expression is the same of Data OFDM symbol:

$$s_n(t) = w_{\Delta T_{SYM}}(t) \sum_{k=-N_{ST}/2}^{N_{ST}/2} d_{k,n} \cdot \exp\left[j2\pi k\Delta f\,(t - T_{GI})\right] \quad (5)$$

where $\Delta T_{SYM} = T_{FFT}+T_{GI}$ = 4μs. Four of the N_{ST}=52 sub-carriers (k=-21,-7,7,21) are dedicated to pilot signals which exploit a pseudo-noise binary sequence of 127 elements cyclically repeated (each sequence element is used for one OFDM symbol). For the Signal symbol, the remaining 48 sub-carriers are always BPSK modulated, while for Data symbols those are dedicated to data according to a specific baseband modulation (BPSK, QPSK, 16-QAM, 64-QAM).

According to the payload size and the exploited coding scheme, different lengths are obtainable for the transmitted frame. In the following we will consider two different cases, the characteristics of which are summarized in Table I.

TABLE I. SIMULATED FRAMES CHARACTERISTICS

	Payload size (bits)	***Data rate***	***Number of OFDM data symbols***	***Frame duration***
Case 1	1000	6Mbps	43	192 μs
Case 2	420	18Mbps	7	48 μs

A software tool has been developed for WiFi OFDM signal simulation according to the above description with random generation of the payload bits. Using the simulated signals, the corresponding AF can be evaluated as in [11]:

$$\Psi(\tau, f_d) = \left|\chi(\tau, f_d)\right|^2 = \left|\int_{-\infty}^{+\infty} s(t)s^*(t+\tau)\exp(j2\pi f_d t)dt\right|^2 \quad (6)$$

where $\chi(\tau,f_d)$ represents the output of the OFDM signal matched filter for delayed and Doppler shifted signal replicas.

The AFs are reported in figures 1-2 for case 1 and case 2, respectively. A coherent integration time of about 0.25 s and a pulsed transmission with a repetition period of 1 ms were considered. In both cases, typical *sinc* structures appear in the Doppler frequency dimension, which are a consequence of the Fourier Transform of a constant module correlation.

With reference to case 1, in the delay dimension the AF is dominated by the AF corresponding to the Data and Signal sub-frames, [7]. It shows a Peak-to-Sidelobe Ratio (PSLR) of 13 dB and a delay resolution (main beam width) equal to $[(N_{ST}+1)\Delta f]^{-1}$ which corresponds to $1/B$=0.06 μs since the subcarriers are spaced so that they span an actual bandwidth B=16.56 MHz. The corresponding equivalent monostatic radar range resolution is given by $\Delta R=c/(2B)$=9.05 m. A range ambiguity appears at τ=3.2 μs, $R=c/(2\Delta f)$=480 m. This is due to the presence of the guard interval T_{GI} inserted for each data OFDM symbol that cyclically extends the FFT output. Nevertheless, this ambiguity is attenuated with respect to the main peak since only a truncated replica of each OFDM symbol is contained in the guard interval ($T_{GI}=T_{FFT}/4$). Notice that, in contrast to the results obtained for the OFDM modulated DTV signals ([6]), the pilots sub-carriers yield a negligible contribution to the global AF, [7].

Depending on the number of data symbols compared to the Preamble sub-frame, the contribution of the latter to the global AF might become significant. In particular, the AF corresponding to the Long Training sequence shows a temporal periodicity for $|\tau|<\Delta T_{LONG}$ with period T_{FFT} since the Long Training sequence consists of $\Delta T_{LONG}/T_{FFT}$=2.5 repetitions of a long training symbol of duration T_{FFT}. This yields range ambiguities at $R=k\cdot(cT_{FFT})/2=k\cdot$480 m ($k$=1,2). Notice that the nearest range ambiguity is coincident with that given by the Data OFDM signal portion. The AF corresponding to the Short Training sequence shows a temporal periodicity for $|\tau|<\Delta T_{SHORT}$ with period $T_{FFT}/4$ since the Short Training sequence consists of $\Delta T_{SHORT}/(T_{FFT}/4)$=10 repetitions of a short training symbol using only 12 sub-carriers with a sub-carrier spacing equal to $4\Delta f$. This yields range ambiguities at $R=k\cdot(cT_{FFT}/4)/2=k\cdot$120 m ($k$=1,...,9) as clearly apparent in Figure 2 which shows the AF obtained after integration of OFDM frames of about 48 μs (shorter Data sub-frame, case 2).

Such isolated peaks in the AF may strongly affect the PBR target detection performance. Particularly, target echoes can be masked by (i) fraction of direct signal received by sidelobe/backlobe of the surveillance antenna, (ii) strong clutter/multipath echoes and (iii) echoes from other strong target even in the presence of large range/Doppler separations.

This masking effect may be counteracted based on two different approaches:

1) by defining effective algorithms for the removal of the undesired contributions in the received signal;

2) by designing proper filters for the control of signal AF sidelobes.

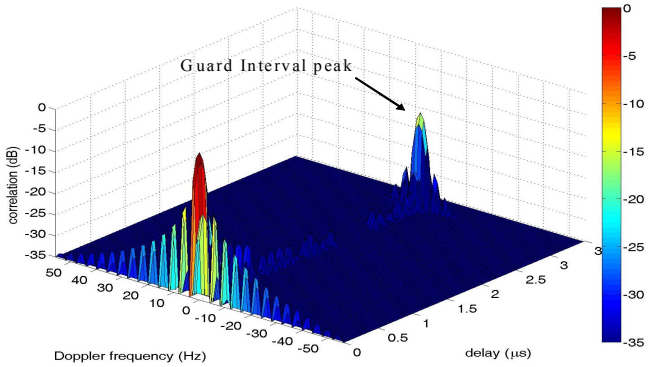

Figure 1 – AF for case 1.

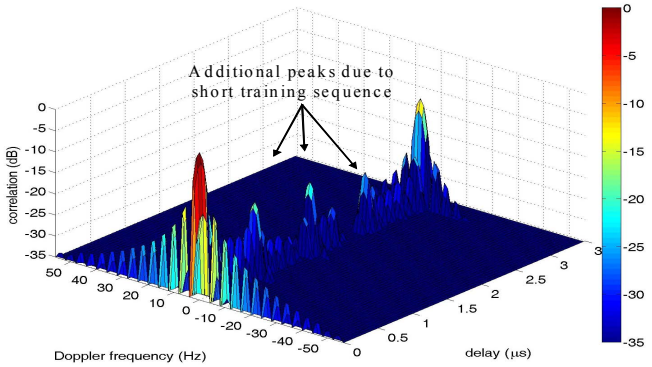

Figure 2 – AF for case 2.

III. Data Processing Steps

A typical PBR processing scheme is sketched in Figure 3. The signal collected at the reference channel is first used to remove undesired contributions on the surveillance channel. After the cancellation stage, the detection process is based on the evaluation of the 2D Cross-Correlation Function (2D-CCF) between the surveillance and the reference signal. In the following we describe the algorithms applied at each processing stage and optimized for the considered application.

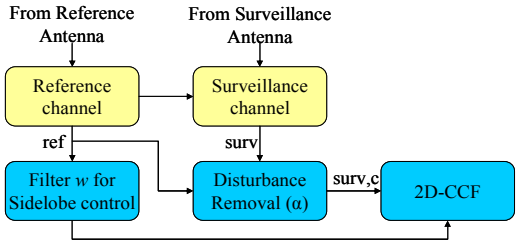

Figure 3 – PBR main data processing steps.

A. Disturbance Removal

Aiming at the detection of moving targets against a stationary background, proper techniques should be implemented to remove the undesired contributions in the surveillance signal (direct signal breakthrough and multipath reflections). To this purpose we resort to the adaptive cancellation approach presented in [12] which operates by subtracting from the surveillance signal properly scaled replicas of the reference signal.

Mathematically, the cancellation stage can be written as:

$$s_{surv,c} = s_{surv} - s_{ref} \otimes \alpha \tag{7}$$

where, $s_{surv,c}$ represents the surveillance signal after disturbance removal, s_{surv} represents the signal collected at surveillance channel, s_{ref} is the reference signal and α represents the cancellation filter. The weights of α are estimated by placing:

$$\min_{\alpha}\{s_{surv} - X\alpha\} \tag{8}$$

where **X** represents a matrix containing delayed versions of s_{ref} corresponding to the range extension on which one want to perform cancellation. For the cancellation filter's weights estimation, Eq. (8) gives:

$$\alpha = \left(X^H X\right)^{-1} X^H s_{surv} \tag{9}$$

Specifically, ECA-B, i.e. the Batches version of the Extensive Cancellation Algorithm, is adopted which requires the filter weights to be estimated over smaller portions of the whole temporal extension over which integration is performed.

Reducing the temporal dimension of the single batch within certain limits does yield significant adaptivity loss when operating in a stationary environment. However, it was demonstrated to make the system more robust to the slowly varying characteristics of the environment which appears to be an appreciable advantage in the considered application.

The performed analysis allowed us to select a batch duration of about 62.5 ms which was experimentally verified to yield a good trade-off between cancellation performance and slow target detection capability.

B. AF Control Filters

As previously mentioned, target detection in a PBR system is mainly based on the evaluation of the 2D-CCF yielding the typical Range-Velocity map. Based on the pulsed nature of WiFi transmissions, this can be achieved by cross-correlating the surveillance signal with the reference signal on a pulse basis and coherently integrating the obtained results over consecutive pulses to achieve the desired Doppler resolution.

According to the analysis presented in the previous section, the detection performance of a WiFi-based PBR may be strongly limited by the strong sidelobe structures appearing in the signal AF which might be responsible for significant masking effects even in the presence of a significant range-Doppler separation.

Aiming at reducing the sidelobes in the Doppler dimension, standard tapering functions can be used when coherently integrating the train of consecutive pulses. However, it is to be noticed that such tapering functions are ineffective against Doppler ambiguities resulting from a large temporal separation between the integrated pulses, namely a low equivalent PRF, which is not within the control of the radar designer. Also we notice that the truly unpleasant sidelobes are the ones at zero delay, where typically no targets is searched for.

In contrast, proper techniques might be designed to reduce the sidelobes of the signal AF in the range dimension. First of all a conventional weighting network in the frequency domain can be applied to improve the PSLR resulting from the rectangular shaped power spectral density (PSD) of the OFDM signal. Aiming at removing the isolated peaks in the zero Doppler cut of the AF due to guard intervals and Short Training Sequence, the approach presented in [13] might be exploited which has been designed for DVB-T-based PBR exploiting an OFDM modulation. According to this approach, the unwanted peaks removal is performed by pre-processing the reference signal with a linear filter based on the knowledge of the expected value of the WiFi OFDM signal Autocorrelation Function (ACF). This can be evaluated based on the analysis presented in [7].

In particular, we observe that the expected value of the ACF is a periodic function with period equal to the symbol duration. This implies that an inverse filter can be designed that is able to whiten the average waveform spectrum. The filter coefficients have a support with the length of a single symbol duration and are obtained directly by the ACF in [7]. By solving a proper inverse filter problem, we obtain:

$$w = FFT\left(\frac{1}{FFT(R)}\right) \tag{10}$$

where R represents the expected ACF. As it is apparent, the filter can be easily applied in the frequency domain by Fourier transforming the input data and then performing the inverse FFT on the filtered data.

Specifically only the ACF values at the peaks locations might be considered to build up the system of linear equations required to obtain the peaks suppression.

As an example, Figure 4 shows the result obtained for the worst case of Figure 2 (very short Data sub-frame) after the application of a Hamming weighting network followed by the approach in [13]. As it is apparent the joint application of the two considered approaches in the range dimension provides a significant improvement of the PSLR and the effective removal of the isolated peaks with only a very limited loss in Signal-to-Noise Ratio (SNR). While the zero-Doppler section in Figure 4 a) shows in details the good performance of the inverse filter, the plot of the AF in Figure 4 b) shows that, after controlling the AF, the whole detection plane is free of spurious sidelobes.

Notice that the Hamming network fails to achieve the theoretical PSLR (>40 dB). This can be explained by recalling that, in OFDM-WiFi system, the central sub-carrier at k=0 is never used thus yielding a "hole" in the corresponding PSD which limits the achievable PSLR to a nominal value of about 27 dB. However, the overall performance of the sidelobe control filter can be considered of a good quality.

The performance of the described processing strategies is analysed in the following Section against a real data set.

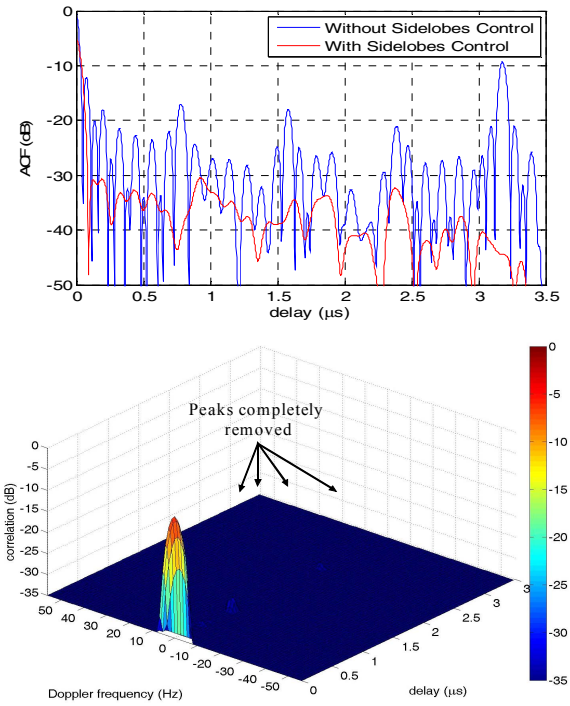

Figure 4 – AF with sidelobe control for a simulated OFDM Frame of 48 μs. a) Zero Doppler cut and b) Entire AF

.

IV. The Experimental Setup

The adopted experimental setup is sketched in Figure 5. For the purpose of our analysis, a portable wireless AP (D-Link DAP 1160) was connected to the transmitting antenna while a -20dB fraction of the transmitted signal was gathered in a dedicated receiving channel (reference channel) by using a directional coupler which yields a 0.5 dB insertion loss and isolation greater than 20 dB. The second channel of a dual-channel receiving system was directly connected to a separate receiving antenna which was used to collect the surveillance signal. The antennas are characterized by a beamwidth of about 15° and a front to back ratio greater than 30dB.

The receiving system uses a single fully coherent down conversion stage for the two channels, so as to move the central frequency of the selected WiFi channel to an intermediate frequency of 15 MHz. After adequate filtering and amplification, the signal is sampled with a sampling frequency equal to 55 MHz using a high quality dual channel A/D converter with a wide dynamic range (software selectable), controlled by an external stable and tunable oscillator.

The acquired IF data was stored and processed off-line using digital filters for the automatic detection of the transmitted pulses and the extraction of the modulated signal complex envelope (digital down-conversion – DDC).

Different tests were performed in an outdoor environment (a parking area in Cisterna di Latina, Italy, see Figure 5) using different targets. For the target detection experiment considered in the following, a quasi-monostatic configuration was adopted for the two antennas which were mounted one on top of the other. Two targets were present (a car and a running man) moving forward in the parking area at approximately 25 km/h. The wireless AP was configured to transmit in channel 7 of the WiFi band (centre frequency of 2.442 GHz), which is a portion of industrial, scientific and medical (ISM) frequency band. It was set up to roam for connected devices emitting a regular Beacon signal exploiting an OFDM modulation at 1 ms intervals. Acquisitions of duration of about 4 sec. were performed consisting of approximately 4000 Beacons.

V. Experimental Results

The target detection performance of the WiFi-based PBR system has been evaluated with reference to the target detection test sketched in Figure 5.

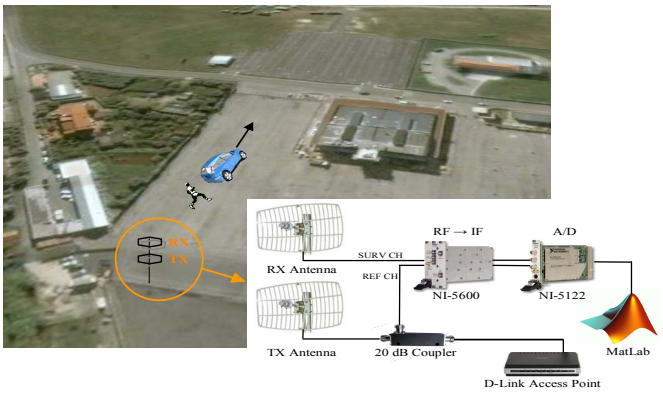

Figure 5 – WiFi experiment area in Cisterna di Latina.

Figure 6 shows the 2D-CCF evaluated, without disturbance cancellation and AF control, over an integration time of 0.25 sec yielding a Doppler resolution equal to 4 Hz (0.88 km/h). The 2D-CCF has been normalized to the nominal thermal noise power level so that the value at each map location represents the estimated SNR.

As it is apparent a strong peak appears at range 15 m and zero velocity corresponding to the direct signal collected by the sidelobes of the receiving antenna (the temporal delay is related to the length of the cables). Due to the high Doppler and range sidelobes, only the strongest target (the car) can be detected while the human target is completely masked.

Figure 7 reports the 2D-CCF evaluated after disturbance cancellation. The cancellation filter operates over consecutive batches of duration 62.5 ms. Moreover, the filter length was set to remove reference signal replicas with delays corresponding to ranges between 0 and 175 meters. As it is apparent the direct signal and all the disturbance contributions at zero Doppler are effectively removed thus significantly increasing the useful dynamic range for target detection. The human target now appears as a peak in the map; however it might be confused with the range sidelobes of the strongest target return. Notice that this masking effect is stressed for increased power level difference between the two targets echoes.

Figure 8 shows the 2D-CCF evaluated without disturbance cancellation but using a mismatched reference signal to achieve the desired sidelobes control. While the sidelobes due

to the direct signal have been significantly reduced, the weakest target detection is still limited by the small dynamic range available. Thus the joint application of the cancellation and the AF control filters is required.

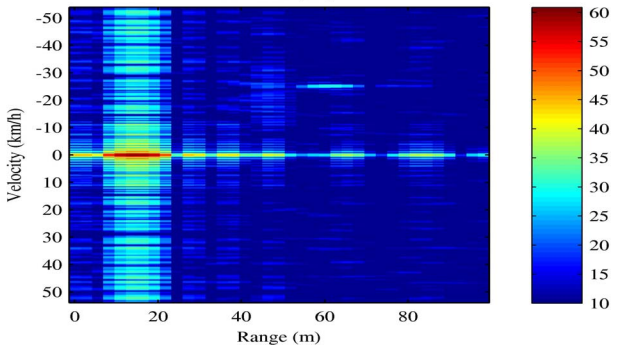

Figure 6 – 2D-CCF without disturbance removal and ACF control.

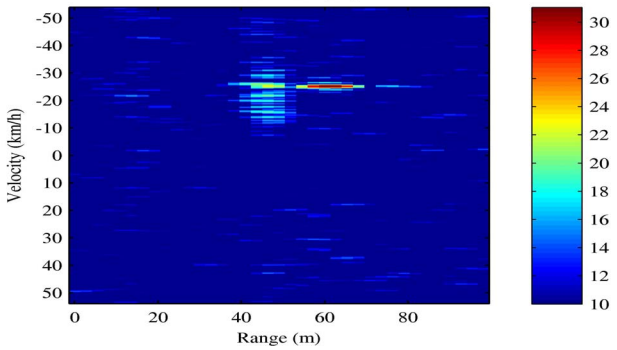

Figure 7 – 2D-CCF with disturbance removal only.

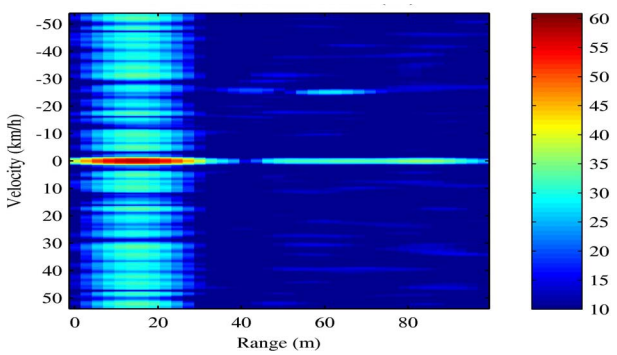

Figure 8 – 2D-CCF with ACF sidelobes control only.

When the 2D-CCF is evaluated after disturbance cancellation using a mismatched reference signal to achieve the desired sidelobes reduction, Figure 9 is obtained.

As it is apparent, two separate peaks are now present in the map at ranges and velocities corresponding to the two targets moving in the parking area so that they can be easily detected without ambiguities. This clearly shows the significant benefit deriving from the joint application of disturbance cancellation techniques and AF control filters despite the small SNR loss to be accepted.

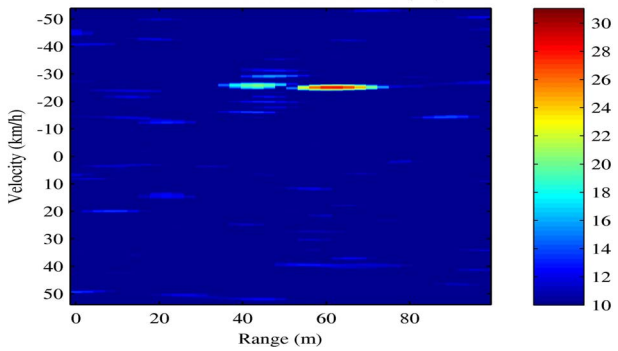

Figure 9 – 2D-CCF with disturbance removal and ACF sidelobes control.

VI. CONCLUSIONS

In this paper the practical feasibility of a WiFi OFDM transmissions based passive bistatic radar (PBR) has been investigated. The required data processing steps have been described for: (i) the control of the signal AF sidelobe level and (ii) the removal of the undesired signal contributions which strongly limit the useful dynamic range. The performance of the conceived techniques has been evaluated with reference to typical signals broadcasted by a IEEE 802.11 AP exploiting a OFDM modulation. The experimental results obtained against a real data set allowed us to preliminary demonstrate the potentialities of a WiFi-based PBR for local area surveillance applications.

REFERENCES

[1] Special Issue on Passive Radar Systems, *IEE Proceedings on Radar, Sonar and Navigation*, vol. 152, Issue 3, pp. 106–223, June 2005.

[2] P. Howland, D. Maksimiuk, and G. Reitsma, "FM radio based bistatic radar," *IEE Proceedings on Radar, Sonar and Navigation*, vol. 152, Issue 3, pp. 107–115, June 2005.

[3] H.D. Griffiths, N.R.W. Long, "Television based bistatic radar", IEE Proc. F, Commun. Radar Signal Process., 1986, 133, (7), pp. 649–657.

[4] G. Fabrizio, F. Colone, P. Lombardo, and A. Farina, "Adaptive beam forming for high frequency over-the-horizon passive radar," *IET Radar, Sonar & Navigation*, Vol. 3, Issue 4, August 2009, pp. 384-405.

[5] C. Coleman and H. Yardley, "Passive bistatic radar based on target illuminations by digital audio broadcasting," *IET Radar, Sonar and Navigation*, vol. 2, Issue 5, Oct. 2008.

[6] R. Saini and M. Cherniakov, "DVT signal ambiguity function analysis for radar application," *IET Proc. on Radar, Sonar and Navigation*, vol. 152, Issue 3, pp. 133–142, June 2005.

[7] F. Colone, K. Woodbridge, H. Guo, D. Mason and C. J. Baker, "Ambiguity Function Analysis of Wireless LAN transmissions for passive radar", in print on *IEEE Trans. on Aerospace and Electronic Systems*.

[8] H. Guo, K. Woodbridge, and C. Baker, "Target detection in high clutter using passive bistatic WiFi radar", in Proc. of IEEE Radar Conference 2009 , 4-8 May 2009, pp. 1–5.

[9] *Wireless LAN Medium Access Control (MAC) and physical Layer (PHY) Specification*, IEEE Std. 802.11, 2007.

[10] P. Falcone, F. Colone, P. Lombardo, T. Bucciarelli, "Range Sidelobes Reduction Filters for WiFi-Based Passive Bistatic Radar", EURAD 2009, Rome, Italy, 30 September-2 October 2009.

[11] Skolnik, M.H., Introduction to radar system, third edition. Boston, MA: McGraw-Hill, 2001.

[12] F. Colone, D. W. O'Hagan, P. Lombardo, C. J. Baker "A multistage processing algorithm for disturbance removal and target detection in Passive Bistatic Radar", *IEEE Trans. on Aerospace and Electronic Systems*, Vol. 45, Issue 2, April 2009, pp. 698-721.

[13] C. Bongioanni, F. Colone, D. Langellotti, P. Lombardo, T. Bucciarelli, "A New Approach for DVB-T Cross-Ambiguity Function Evaluation", EURAD 2009, Rome, Italy, 30 September-2 October 2009.